ELSEVIER

Journal of Alloys and Compounds 325 (2001) 194–200

Journal of ALLOYS AND COMPOUNDS

www.elsevier.com/locate/jallcom

Directional solidification and characterization of binary Fe–Pr and Fe–Nd eutectic alloys

I.A. Santos[a,*], A.A. Coelho[b], R.C. Araújo[b], C.A. Ribeiro[b], S. Gama[b]

[a]*Departamento de Física, Universidade Federal de São Carlos, Caixa Postal 676, 13565-670 São Carlos, SP — Brazil*
[b]*Instituto de Física Gleb Wataghin, Universidade Estadual de Campinas - UNICAMP, Caixa Postal 6165, 13083-970 Campinas, SP — Brazil*

Received 3 January 2001; accepted 6 April 2001

Abstract

In this work, the directional solidification technique was employed in binary Fe–Pr and Fe–Nd eutectic alloys with compositions near to their respective eutectic points. Solidifying the Fe–Pr and Fe–Nd hypereutectic alloys in a vertical Bridgman crystal growth unit, we were able to obtain the two eutectic morphologies, one globular and other feathered, normally observed in as-cast samples, in a coarser form and sequentially displayed along the length of the samples. The transition temperatures nearby to the eutectic points were also determined using a Calvet type calorimeter. The phases comprising the globular and feathered morphologies were determined as being, respectively, $Fe_{17}R_2$ and Fe_2R (R=Pr or Nd), for both systems. These experiments also showed very clearly the peritectic formation of the Fe_2R phases from the $Fe_{17}R_2$ and the liquids. Thermomagnetic measurements gave the Curie temperature as being 44°C for the Fe_2Pr phase and 252°C for the Fe_2Nd phase.

Keywords: Transition metal alloys; Rare earth alloys; Microstructure; Calorimetry

1. Introduction

In the last years, the utilization of the directional solidification of eutectic alloys has been employed in a considerable number of experimental and theoretical investigation [1]. The eutectic directional solidification provides us microstructures with the simultaneous formation of two solid phases from one determined liquid, i.e. the phases of interest are obtained directly from the melt. The phase relations for the binary Fe–Pr and Fe–Nd systems have been of great interest since the discovery of the $Fe_{14}Nd_2B$ compound [2]. The Fe–Pr system has an important advantage over the Fe–Nd system, whereas the process for permanent magnet manufacture with the $Fe_{14}Nd_2B$ compound depends of the powder metallurgical process, while the magnets prepared with the $Fe_{14}Pr_2B$ compound can be obtained directly from the melt [3]. The understanding of the phase relations around the eutectic region of these binary systems is important because the binary eutectic liquid plays an important role in the overall magnetic performance of the magnets based on these rare earths metals [4,5].

The experimental studies of alloys around the eutectic compositions of these binary systems showed that in alloys frozen quickly, metastable phases are observed and formed with an eutectic morphology, being easily identified through metallographic analysis [6–8]. These phases are magnetically ordered and are greatly modified by annealing. The structural changes of these phases into $Fe_{17}Pr_2$ or $Fe_{17}Nd_2$ phases promote remarkable alterations in the magnetic properties of the alloys, particularly in their coercivity [5,9,10]. In these systems, simultaneously with the formation of these magnetic metastable phases [11], two thermal events were observed in Differential Thermal Analysis (DTA) measurements around the R-rich eutectic [5]. For the as-cast samples, the eutectic always shows a very fine microstructure, with at least two morphologies, one of them termed ‘feathered’ and the other ‘globular’ [6,10]. Measurements of hysteresis cycles showed that as-cast alloys, containing substantial eutectic amounts, present high coercive fields. The phase responsible for the magnetic properties has Curie temperature around 230°C and is metastable under 600°C heat-treatments [12,13]. Due to its very fine morphology, it was not possible to determine the stoichiometry of this ordered phase (termed P1) [5,6]. It was assumed that a metastable ordered phase is formed during the solidification of the eutectic liquid.

*Corresponding author.
E-mail address: pias@iris.ufscar.br (I.A. Santos).

0925-8388/01/$ – see front matter
PII: S0925-8388(01)01394-9

Thus, a metastable eutectic reaction $L+R\rightarrow(R+P1)_{eutectic}+(R)$, where R=Pr or Nd, occurs simultaneously with a second eutectic $L+R\rightarrow(R+Fe_{17}R_2)_{eutectic}+(R)$. The first eutectic would give origin to the feathered morphology and the second to the globular one. It was clear that the study of the phase relations in this region of the phase diagrams would require experimental techniques able to cope with phenomena occurring in a small temperature interval and able to produce morphologies coarser than the ones obtained in the usual melting procedures.

The objective of this work is to report results obtained in directional solidification (DS) of the alloys with compositions near to the Fe–Nd and Fe–Pr eutectic compositions. The samples were obtained and studied using DS and very slow Calvet-type calorimetric measurements. The microstructure characteristics of the phases observed in the eutectic region, as well as some of their magnetic properties, were determined through metallography and thermomagnetic analysis.

2. Experimental procedure

The samples were obtained by arc-melting appropriate proportions of 99.99% pure iron, 99.9% pure praseodymium and 99.9% pure neodymium (Aldrich). The metals, as well as the synthesized alloys, are always kept stored under controlled argon atmosphere to avoid any oxidation. The arc-melting procedure consists in fusing the precursor metals directly into the arc-furnace. During this process, the samples have their position reversed many times in the crucible (between successive fusion) to guarantee that the metals components had been mixed homogeneously. For the DS experiments, samples were placed in cylindrical CaF_2 crucibles obtained by the methods previously reported in the literature [14]. The choice of these crucibles is justified because there are no contamination of the ingots by calcium fluoride. Directional solidification was made for compositions with 15 at. % Fe and 85 at. % Pr (hereinafter denominated 15Fe–85Pr) and 20 at. % Fe and 80 at. % Nd (hereinafter denominated 20Fe–80Nd) in a radio frequency (RF) furnace. For doing the DS experiments a vertical Bridgman crystal growth unit was used. A furnace with a variable coil, which promotes a convenient temperature gradient, composes this crystal growth unit. As a susceptor, we used a tantalum tube held in place by a niobium holder and quartz tubes. For all experiments, the furnace was evacuated down to 10^{-6} Torr and then filled with high purity argon up to 4 atm. This procedure is necessary to prevent the contamination of the samples due to their high reactivity, once they are rich in the rare earth elements. During the DS runs the temperature was monitored using a Leeds and Northrup optical pyrometer. Cooling rates, measured as the speed of the vertical movement of the crucible, were 1, 10 and 20 mm/h. In this way, the DS duration was 50, 5 and 2.5 h. Samples of typically 50 mm in length and 8 mm in diameter were obtained employing this procedure. The DS technique makes microstructures that change along samples length according to the cooling sequence expected from the phase diagrams (no radial changes were observed). Thus, the directionally solidified samples were divided in two parts: the inferior part (the first that solidifies) and the upper part (the last one to be solidified). This division is valid for all the characterization techniques employed in this work. Our calorimetric experiments were made in a Calvet type calorimeter; model HT1000D, from Setaram, run in the scanning mode. The scanning rate used for most of our experiments was 0.05°C/min in the temperature range of interest. All samples directionally solidified and run in the calorimeter were characterized by metallography. Some of these samples were analyzed in an electron microprobe in order to determine the chemical composition of the formed phases. In order to determine the Curie temperature of the phases contained in the samples, we did AC susceptibility measurements in a homemade Thermomagnetic Analyzer (TMA) as previously described [15].

3. Results and discussion

The microstructure of as-cast 30Fe–70Pr and 25Fe–75Nd samples, obtained by arc-melting, are shown in Fig. 1. Fig. 1a shows the microstructure of the 30Fe–70Pr sample and Fig. 1b shows the microstructure of the 25Fe–75Nd sample. These alloys composition are situated in the hypoeutectic region of the corresponding phase diagrams for both systems [8]. In these figures, it can be observed two typical eutectic morphologies previously cited, the feathered (1) and globular (2) structures, and probably the $Fe_{17}Pr_2$ or $Fe_{17}Nd_2$ phases (3). This is the typical microstructure of the samples of these systems solidified at high cooling rates, as the ones proportioned by arc-melting. The microstructural morphologies for both materials are very similar, however the TMA signals are very different. For the binary Fe–Pr system case, it can be observed a strong signal around 204°C corresponding to the so-called P1 phase [6,7] together a similarly strong signal corresponding to the $Fe_{17}Pr_2$ phase, as shown in Fig. 2a (30Fe–Pr70 as-cast sample). As it can be seen in Fig. 2b, the amount of this phase decreases as the 15Fe–Pr85 sample is DS at 1 mm/h (superior part), and a phase with a T_c of 44°C starts to appear in the TMA signal. This phase was characterized as being the Fe_2Pr phase and will be discussed below regarding the DS samples characteristics. In the binary Fe–Nd system case, a strong signal corresponding to the $Fe_{17}Nd_2$, and two other signals that correspond to the γ (at 166°C) stable phase and the P1 (at 242°C) metastable phase [16], can be observed (Fig. 3a, as-cast 25Fe–75Nd sample). When the 20Fe–80Nd sample is DS at 1 mm/h (superior part), the signals of the $Fe_{17}Nd_2$

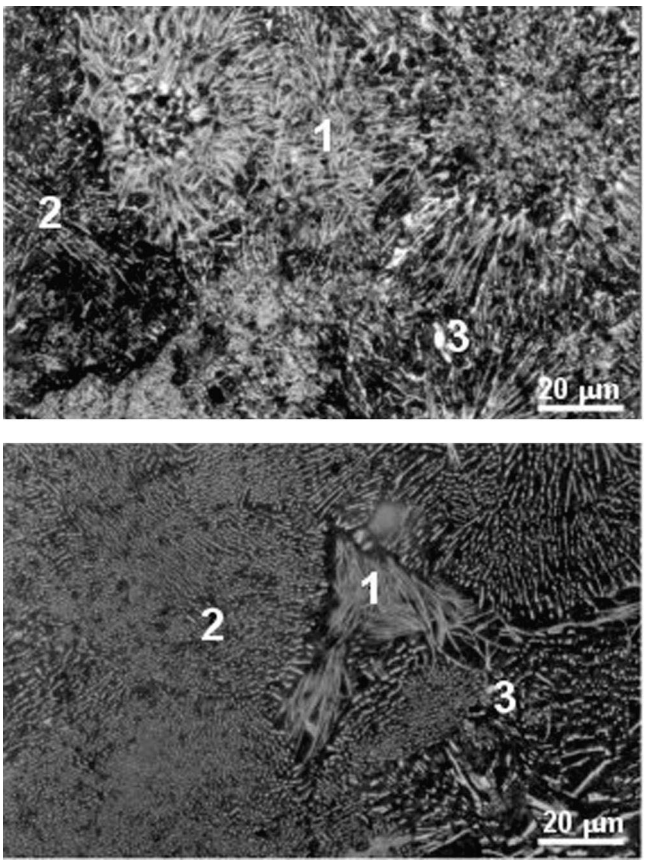

Fig. 1. Microstructures of the (a) 30Fe–70Pr and (b) 25Fe–75Nd samples obtained by arc-melting (500×). (1) feathered, (2) globular and (3) $Fe_{17}R_2$ (R=Pr or Nd)).

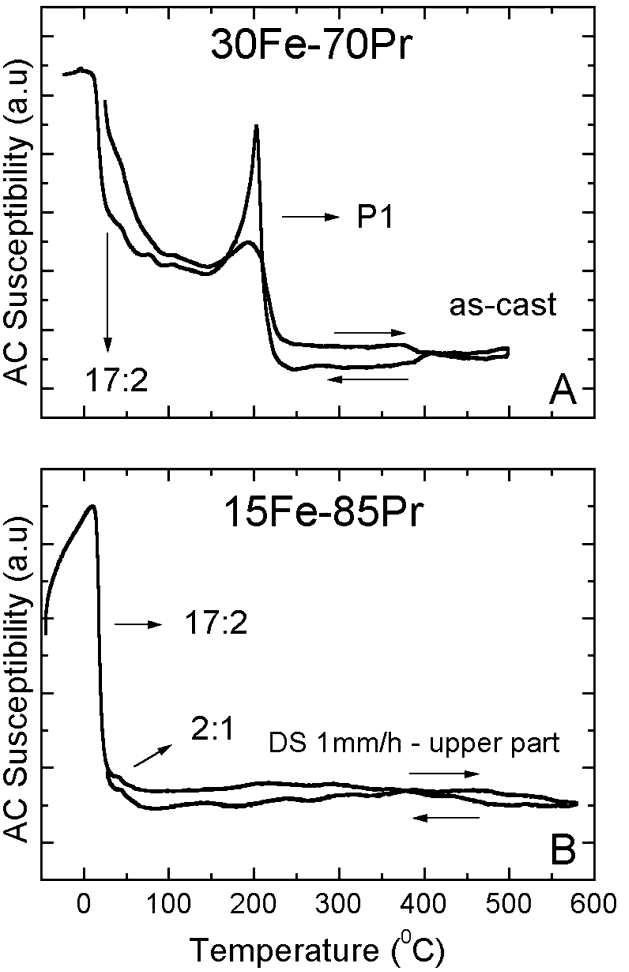

Fig. 2. (a) TMA characteristics of 30Fe–70Pr sample as-cast in arc-furnace. (b) TMA characteristics of the 15Fe–Pr85 sample DS at 1 mm/h (superior part). For details see text.

and γ phases emerge together with a new signal at 252°C, as shown in Fig. 3b. This latter signal was related to the Fe_2Nd phase, which will also be discussed below considering the DS samples characteristics.

All the directionally solidified samples showed similar microstructures, differing only in the coarseness of the formed phases as the cooling speed decreased. In both systems, the globular eutectic morphology was observed majority in the inferior parts of the ingots, while the feathered eutectic morphology was observed majority in the superior parts.

It is interesting to note that in DS samples the first part to cool displays the globular morphology, while the superior part shows essentially the feathered morphology, as if there is a sequence of the two eutectic morphologies previously cited. These DS microstructures, now presenting the phases with sizes big enough to identify them unambiguously, where carefully analyzed. Through metallographic and microprobe analysis, we identified the phase comprising the globular morphology as being the $Fe_{17}R_2$ and the phase comprising the feathered morphology as Fe_2R with high confidence in both systems. We also observed the Fe_2R phases in a peritectic morphology with the $Fe_{17}R_2$ and (R-rich) phases. As it can be seen in Fig. 4, the Fe_2R phases seem to be stable, being formed peritectically from the liquids and $Fe_{17}R_2$ phases. The peritectic reaction, which is responsible for the formation of the Fe_2Pr phase, is shown in Fig. 4a, where the superior part of the 15Fe–85Pr sample obtained by DS, run at 10 mm/h, is analyzed. We see clearly that the 2:1 phase is formed peritectically from the 17:2 phase and liquid. A similar peritectic reaction for the Fe_2Nd phase in the Fe–Nd system, obtained under similar experimental conditions solidifying the 20Fe–80Nd sample, is shown in Fig. 4b. These results point to the interpretation that, which the very low cooling rates achieved in DS experiments, we have first a peritectic reaction described as: $Fe_{17}R_2 + L \rightarrow (Fe_{17}R_2 + Fe_2R)_{peritectic} + L$, followed by the eutectic reaction described as: $L + Fe_2R \rightarrow (Fe_2R + R)_{eutectic} + Fe_2R$. The globular eutectic morphologies, which are solidified in the inferior part of the ingots, and comprise the $Fe_{17}R_2$ phases, are probably provenience of an eutectoid decomposition of the Fe_2R phases, and can be described as: $Fe_2R + (R) \rightarrow (Fe_{17}R_2 + R)_{eutectoid} + (R)$.

This reaction sequences and the interpretation of the

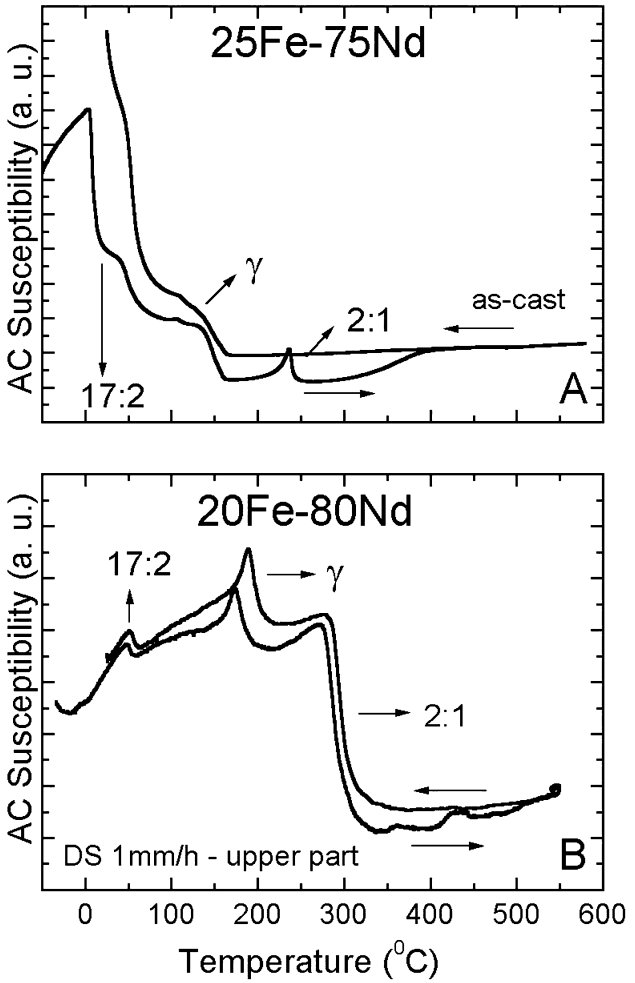

Fig. 3. (a) TMA characteristics of 25Fe–75Nd sample as-cast in arc-furnace. (b) TMA characteristics of the 20Fe–Nd80 sample DS at 1 mm/h (superior part). For details see text.

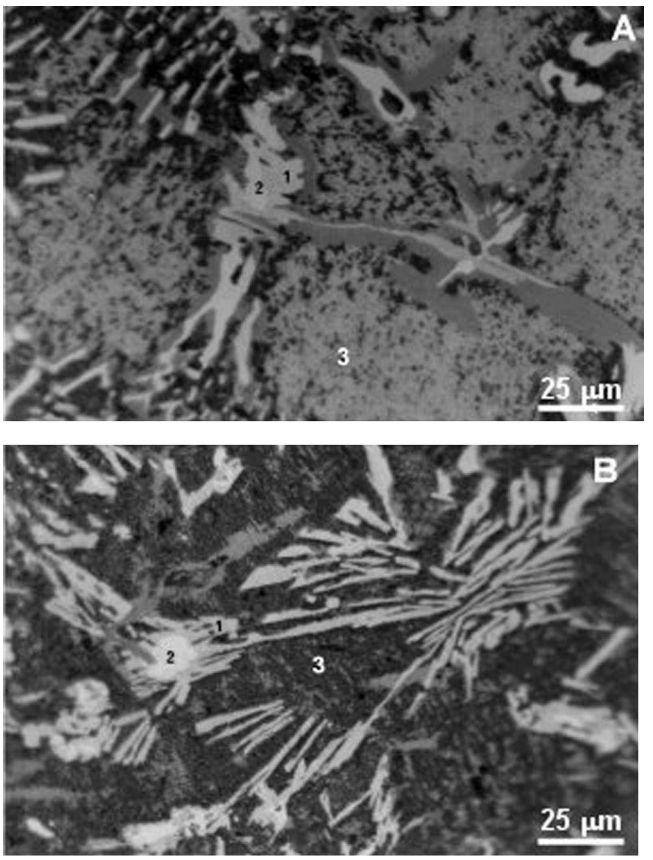

Fig. 4. Microstructures of the (a) 15Fe–85Pr and (b) 20Fe–80Nd samples obtained by directional solidification at solidification rate of 10 mm/h (400×). (1) Fe_2R–peritectic formation (2) $Fe_{17}R_2$ and (3) R-rich phase (R=Pr or Nd).

sequence of microstructures obtained by DS experiment can be clearly confirmed by calorimetric analysis in hypoeutectic and hypereutectic alloys. Calorimetric analysis of the 30Fe–70Pr and 25Fe–75Nd (hypoeutectic) alloys reveals the existence of two thermal events in both systems (Figs. 5a and 6a). For the Fe–Pr system, they occurred at 664°C and 669°C (being both temperature averages of several runs), and can be respectively associated to the eutectic and peritectic reactions above cited. For the Fe–Nd system, the thermal events observed at 682°C and 688°C, can also be respectively associated to the peritectic and eutectic reactions of this system. However, calorimetric analysis of the 15Fe–85Pr (Fig. 5b) and 20Fe–80Nd (Fig. 6b) hypereutectic alloys reveals only one thermal event at 664°C, for the Fe–Pr system, and 682°C, for the Fe–Nd system. As can be concluded, these thermal events are associated to the respective eutectic reactions in both binary systems.

The microstructural characteristics of these phases can point the following interpretation: the solidification of hypoeutectic alloys, prepared near the eutectic point, produces the peritectic formation of the Fe_2R phases from the liquids and $Fe_{17}R_2$ phases. This reaction are followed by the eutectic reactions comprising Fe_2R and (R) phases. Finally, with decreasing the temperature, the eutectoid reactions comprising the $Fe_{17}R$ and (R) phases can be hypothesized. This sequence of the reactions induces the misinterpretation, generally made through metallographic analysis in as-cast samples, of the existence of eutectic reactions comprising the $Fe_{17}R_2$ and the (R) phases. Indeed, the eutectoid decomposition reaction involving the Fe_2Nd phase for the Fe–Nd system was recently reported in the literature [16]. In this way, the globular morphology can be associated to the eutectoid reaction described above. And also, the solidification of the alloys, with hypereutectic compositions close to the eutectic points, produces directly the eutectics comprising the Fe_2R and (R) phases, followed by the eutectoids decomposition of the Fe_2R phases as described previously. In this way, the feathered morphology can be associated to the eutectic reactions: $L+Fe_2R \rightarrow (Fe_2R+R)_{eutectic}+Fe_2R$ and the globular morphology can be associated to the eutectoid reactions: $Fe_2R+(R) \rightarrow (Fe_{17}R_2+R)_{eutectoid}+(R)$.

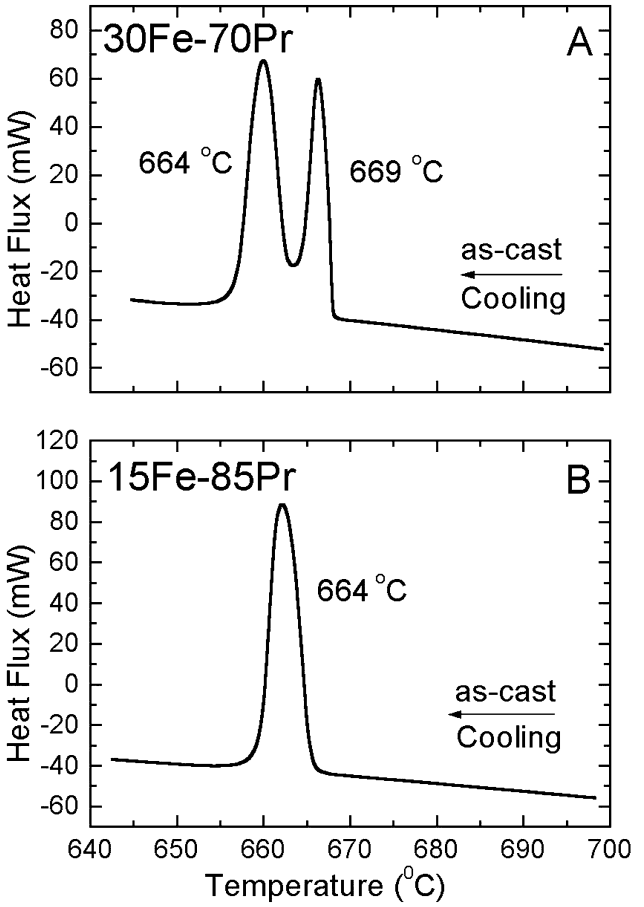

Fig. 5. Calvet measurement of the (a) 30Fe–70Pr and (b) 15Fe–85Pr samples at 0.05°C/min. The signal at 669°C corresponds to the peritectic formation of the Fe_2Pr phase and the signal at 664°C is the eutectic reaction $L+Fe_2Pr \rightarrow (Fe_2Pr+Pr)_{eutectic}+Fe_2Pr$.

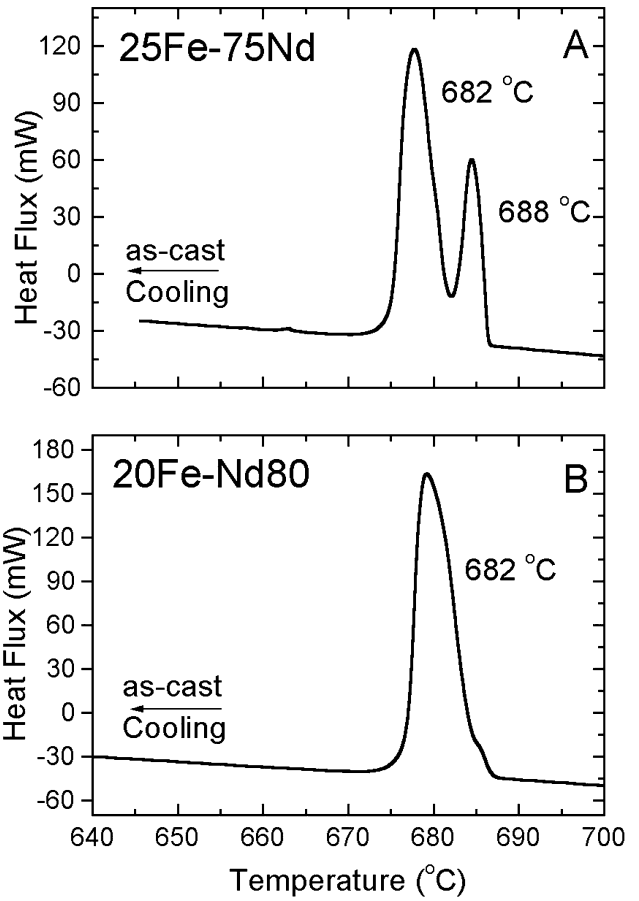

Fig. 6. Calvet measurement of the (a) 25Fe–75Nd and (b) 20Fe–80Nd samples at 0.05°C/min. The signal at 688°C corresponds to the peritectic formation of the Fe_2Pr phase and the signal at 682°C is the eutectic reaction $L+Fe_2Nd \rightarrow (Fe_2Nd+Nd)_{eutectic}+Fe_2Nd$.

It is necessary to discuss the relation between the above-mentioned P1 (usually observed in as-cast alloys) and Fe_2R phases (usually observed in DS or calorimeter runner samples). In the Fe–Pr system case, the as-cast samples present the P1 phase with a T_c of 204°C (Fig. 2a), while all the DS samples present the Fe_2Pr phase with a T_c of 44°C (see Fig. 2b). What is remarkable is that the morphological characteristics, revealed by metallographic analysis, indicate that P1 phase is the 2:1 phase, whereas P1 phase is found in the feathered morphology of the as-cast alloys and Fe_2Pr is found in the feathered morphology of the DS alloys. In fact, as the DS cooling rates increase, the similarities between the samples morphologies increase, explained by the fact that, in this case, the solidification rates of the DS and arc-furnace equipment would tend to be the same (compare Figs. 1A, 4A and 7A). Other evidences in the literature confirmed, by microdiffraction and microprobe analysis [17], and still by TMA and metallographic analysis [18], them as identical. Thus, it is tempting to conclude that the P1 phase in Fe–Pr system is the Fe_2Pr phase, and that it undergoes, at constant composition, a structural (crystallographic) transition, changing its T_c from 204°C down to 44°C. This proposed solid state reaction can be due to the long time high temperature exposure of the slowly DS samples. In the Fe–Nd system case, the TMA measurements in DS samples indicate the presence of the same phases found in the arc-melting samples (Fig. 3). We observe a slight variation in the value of the Curie temperatures of the P1 and Fe_2Nd phases as we go from the as-cast to the DS samples — it changes from 242°C to 252°C. Nevertheless, the metallographic analysis showed both P1 and Fe_2Nd phases with the feathered morphology (compare Figs. 1B, 4B and 7B). This evidence, as well as others in the literature [16], confirms them as the same, as in Fe–Pr system case.

In both systems, a third phase was observed by metallographic analysis. The stoichiometry of them was not determined due to its reduced size. These phases are mainly viewed in samples obtained in DS experiments run at solidification rates of 20 mm/h. They are showed in Fig. 7 (indicated by the letters E). It is interesting to note that the microstructures of the samples solidified at higher solidification rates are very similar to the samples obtained

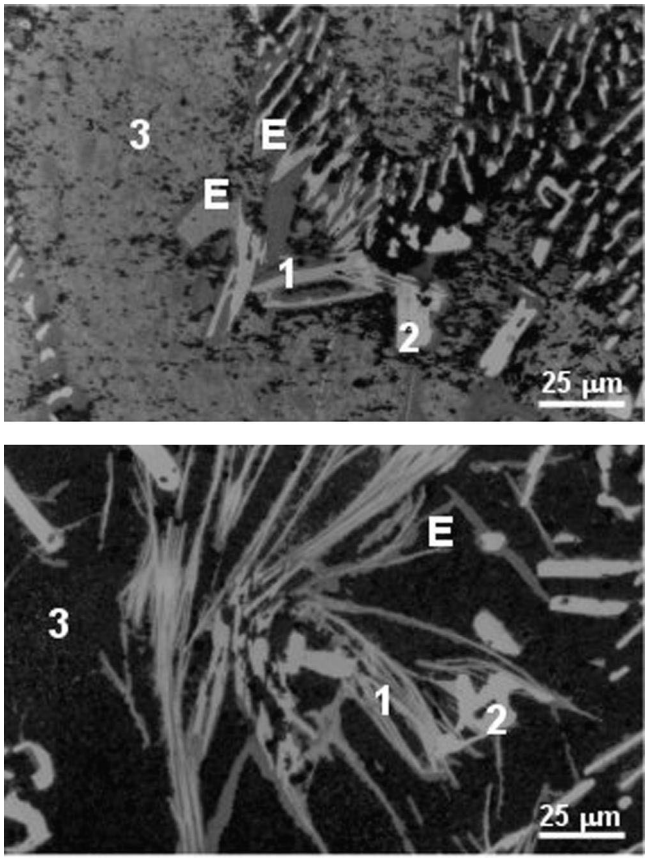

Fig. 7. Microstructures of the (a) 15Fe–85Pr and (b) 20Fe–80Nd samples obtained by directional solidification at solidification rate of the 20 mm/h (400×). The letters **E** in the illustrations indicate the unidentified phases observed in quickly solidified samples of both systems. (1) Fe_2R, (2) $Fe_{17}R_2$ and (3) R-rich phase.

by arc-melting (compare, for example, Figs. 1b and 7b). This is a clear evidence that the directional solidification technique is appropriate to induce big sizes of the phases that are ordinarily obtained only in small sizes in these complex systems. Moreover, in samples solidified at lower solidification rates, the presence of the metastable phases is inhibited.

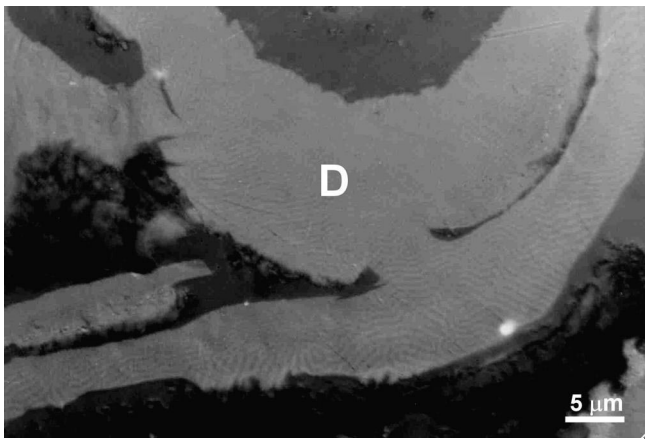

Fig. 8. Microstructure of the 20Fe–80Nd directional solidified (1 mm/h) sample, showing magnetic domains of the Fe_2Nd phase (D) (500×).

In a sample containing almost only the Fe_2Nd phase (superior part of the 20Fe–80Nd DS sample at 1 mm/h) it can be clearly observed the presence of ferromagnetic domains (revealed under polarized light), which indicate that this phase is magnetically axially ordered (Fig. 8). The Fe_2Pr phase does not show this characteristic, i.e. the Fe_2Pr phase seems to be not axially ordered. However, this lack of domains can be because its Curie temperature is very close to the ambient temperature. Researches concerning the true magnetic ordering of these phases are in progress and will be published elsewhere.

4. Conclusions

Using the directional solidification and Calvet-type calorimetric techniques in Fe–Pr and Fe–Nd alloys with compositions nearby the eutectic point, we were able to obtain the two characteristics eutectic morphologies normally observed in as-cast samples in a coarser form and displayed along the length of the samples. The obtained phase sizes were sufficiently big to allow a very precise determination of their stoichiometry. The feathered morphology was identified as being the Fe_2Pr phase, for the Fe–Pr system, and the Fe_2Nd phase for the Fe–Nd system. These experiments also showed very clearly the peritectic formation of these phases, which can be generically described as: $Fe_{17}R_2+L\rightarrow(Fe_2R+R)_{peritectic}+L$. In this way, their eutectoid decomposition into $Fe_{17}R_2$ and (R) phases was proposed. In the experiments performed at higher solidification rates, we observed the formation of metastable phases whose compositions could not be determined due to its small sizes. As the directional solidification rate is increased, the obtained microstructures become more similar to the microstructures obtained by arc-melting. Nevertheless, our observations indicate the presence of fine magnetic domains in the Fe_2Nd phase at ambient temperature, while they are absent in the Fe_2Pr phase, however, this can be due to the fact that its Curie temperature is too close to the observation (ambient) temperature. The magnetic domains are an indication that the Fe_2Nd phase can be magnetically axially ordered.

Acknowledgements

The authors gratefully thank the Brazilian agencies CNPq and FAPESP for the financial support.

References

[1] R. Trivedi, J.T. Mason, J.D. Verhoeven, W. Kurz, Met. Trans. 22A (1991) 2523.

[2] M. Sagawa, S. Fujimura, N. Togawa, H. Yamamoto, Y. Mitsuura, J. Appl. Phys. 55 (1984) 2083.
[3] F.Z. Lian, F. Pourarian, S. Shimizu, S.G. Sankar, W.R. Wallace, J. App. Phys. 75 (1994) 6289.
[4] G. Schneider, F.J.G. Landgraf, F.P. Missell, J. Less-Common Met. 153 (1989) 169.
[5] F.J.G. Landgraf, G. Schneider, V. Villas-Boas, F.P. Missell, J. Less-Common Met. 163 (1991) 209.
[6] F.A.O. Cabral, S. Gama, J. Less-Common Met. 167 (1990) 31.
[7] F.A.O. Cabral, PhD. Thesis, IFGW-Unicamp, SP — Brazil, 1991 (in portuguese).
[8] O. Kubaschewski, Iron Binary Phase Diagrams, Springer Verlag, 1982.
[9] G. Schneider, F.J.G. Landgraf, V. Villas-Boas, G. Bezerra, F.P. Missell, A.E. Ray, Mat. Lett. 8 (1989) 472.
[10] F.A.O. Cabral, S. Gama, IEEE Trans. Magn. 26 (1990) 1930.
[11] J.L. Sánches-Llamazares, F. Calderon, F. Bolzoni, F. Leccabue, H.H. Xue, J.P. Nozières, J. Magn. Magn. Mat 86 (1990) 307.
[12] F.J.G. Landgraf, F.P. Missell, G. Knoch, B. Grieb, E.-Th. Henig, J. Appl. Phys. 70 (1991) 6107.
[13] J.F. Cannon, D.L. Robertson, H.T. Hall, Mat. Res. Bull. 7 (1972) 5.
[14] A.A. Coelho, S. Gama, C.A. Ribeiro, N.L. Sanjurjo, Ch.V. Mohan, H. Kronmüller, J. Crys. Growth 171 (1997) 125.
[15] E. de Morais, S. Gama, A. Urbano, G.A. Garcia, F.A.O. Cabral, IEEE Trans. Mag. 32 (1996) 4929.
[16] I.A. Santos, S. Gama, J. Appl. Phys. 86 (1999) 2334.
[17] E.V. Obrucheva, B.V. Jalnin, V.P. Menushenkov, A.M. Gabay, in: Proc. 9th Int. Symp. Magnetic Anisot. and Coerc, Rare-earth Trans. Met. Alloys, Vol. 2, 1996, p. 142.
[18] I.A. Santos, A.A. Coelho, S. Gama, J. Appl. Phys., in press.